International Journal of Geo-Information

MDPI

Article

Observational Analysis of Variation Characteristics of GPS-Based TEC Fluctuation over China

Xifeng Liu [1,2,*], Yunbin Yuan [1,*], Bingfeng Tan [1,2] and Min Li [1,2]

[1] State Key Laboratory of Geodesy and Earth's Dynamics, Institute of Geodesy and Geophysics, Chinese Academy of Sciences, Wuhan 430077, China; bingfengtan@whigg.ac.cn (B.T.); limin@whigg.ac.cn (M.L.)

[2] University of Chinese Academy of Sciences, No. 19A Yuquan Road, Beijing 100049, China

* Correspondence: lxf@whigg.ac.cn (X.L.); yybgps@whigg.ac.cn (Y.Y.); Tel.: +86-159-2751-3503 (X.L.)

Academic Editors: Zhao-Liang Li, Jose A. Sobrino and Wolfgang Kainz

Received: 19 September 2016; Accepted: 1 December 2016; Published: 8 December 2016

Abstract: In this study, the characteristics of the total electron content (TEC) fluctuations and their regional differences over China were analyzed by utilizing the rate of the TEC index (ROTI) based on GPS data from 21 reference stations across China during a solar cycle. The results show that there were significant regional differences at different latitudes. Strong ionospheric TEC fluctuations were usually observed at lower latitudes in southern China, where the occurrence of TEC fluctuations demonstrated typical nighttime- and season-dependent (equinox months) features. This phenomenon was consistent with the ionospheric scintillation characteristics of this region. Additionally, compared to low-latitude China, the intensity of TEC fluctuations over mid-latitude China was significantly weaker, and the occurrence of TEC fluctuations was not a nighttime-dependent phenomenon. Moreover, the intensity of TEC fluctuations was much stronger during high solar activity than during low solar activity. Furthermore, the summer-dependent characteristics of TEC fluctuations gradually emerged over lower mid-latitude areas as equinox characteristics weakened. Similar to the equinox characteristics, the summer-dependent characteristics gradually weakened or even disappeared with the increasing latitude. Relevant discussions of this phenomenon are still relatively rare, and it requires further study and analysis.

Keywords: Crustal Movement Observation Network of China (CMONOC); Total Electron Content (TEC); Rate of TEC (ROT); Rate of TEC Index (ROTI)

1. Introduction

As one of the earliest known effects of space weather, ionospheric irregularities have a great impact on the Global Navigation Satellite System (GNSS) and satellite communication [1–6] because they can result in rapid random fluctuations or degradation of the signal amplitude, phase and delay. Moreover, ionospheric scintillations can simultaneously accompany the occurrence of cycle slips or the complete loss of lock on GNSS signals. Similarly affected by irregular ionospheric activities, GNSS has become a powerful tool for investigating the total electron content (TEC) and TEC fluctuations associated with irregular ionospheric activities along signal paths [7–15], which have become essential to the way we live and work [16–20].

Two common parameters, the amplitude/phase scintillation index S_4/σ_ϕ and ROTI, are typically used to quantitatively describe the intensity of ionospheric scintillations or TEC fluctuations. Measurements of both S_4 and σ_ϕ can be derived from GNSS scintillation monitoring receivers sampled at high frequencies, but the number and regional/global distribution of scintillation monitoring receivers are limited due to high costs. This sparsity of scintillation monitoring receivers restricts the extensive use of S_4/σ_ϕ indices [7,9–12].

The TEC fluctuation index ROTI (which is derived from ordinary non-scintillation GNSS receivers sampled at low frequencies) was first proposed by Pi et al. [7,11] in 1997. Since then, it has been widely used to detect irregular ionospheric activities, which are defined as the standard deviation of the rate of TEC (ROT) in a given 5 min interval. Previous studies have demonstrated close correlations between ROTI and scintillation indices [7,15,21,22]. Over the past two decades, ROTI has been widely used to detect regional and global TEC fluctuations, especially with the growing number of GNSS tracking sites [7–13,23–25].

China, which is situated at low and middle latitudes, is a suitable choice for conducting studies on irregular ionospheric activities, owing to the complexity and variability in ionospheric structures over this country. During the past two decades, many scholars have investigated and studied the ionospheric scintillations relevant to irregularities over the north crest of the equatorial anomaly region in southern China [15,22,26–39]. These studies revealed variations in temporal and spatial characteristics in ionospheric scintillations. Deng et al. [26,27] investigated the statistical features of ionospheric scintillations derived from GPS satellites over south China and discussed the close correlations among TEC depletion, scintillation, and ROTI. Liu et al. [33] analyzed the equinoctial behaviors of ionospheric plasma density during low solar activity and revealed the phenomenon of equinoctial asymmetry in ionospheric plasma density. Shi et al. [37] analyzed the close relationship between strong range spread F and ionospheric scintillation over Hainan; their correlation coefficient was as high as 0.93. Yang et al. [22] discussed the close relationship between ROTI and the scintillation indices over Hong Kong. Li et al. [15] investigated the ratio of ROTI to the amplitude scintillation indices over Sanya and showed that it varied between 0.3 and 6.0.

However, previous investigations on the characteristics of irregular ionospheric activities over China have been insufficient because of the restrictions over the lower latitudes in China. Thus, in this study, ROTI indices were used to investigate the characteristics of ionospheric TEC fluctuations, varying with local time (LT) and season, and their regional differences over China during a solar cycle (the 11-year pattern from 2002 to 2012).

2. Methods and Data Processing

In 1997, Pi et al. [11] proposed the rate of the TEC index (ROTI, in TECU/min) to describe the measurements of ionospheric irregularity and scintillation activity. The rate of TEC (ROT, in TECU/min) is measured by utilizing dual-frequency GPS observation phase data, and computing the relative TEC changes, epoch by epoch, along the signal paths from each individual to the receiver, as shown in Equation (1). The index ROTI is defined as the standard deviation of ROT over a 5 min time interval, as shown in Equation (2).

$$\mathrm{ROT} = \frac{\Delta STEC}{\Delta t} \tag{1}$$

$$\mathrm{ROTI} = \sqrt{\left\langle \mathrm{ROT}^2 \right\rangle - \langle \mathrm{ROT} \rangle^2} \tag{2}$$

where $STEC$ represents the TEC along the ray path from the satellite to the receiver (in TECU) and Δt (in seconds) denotes the sampling interval.

In this study, dual-frequency GPS data are provided by the Crustal Movement Observation Network of China, and 21 continuously operating GNSS tracking stations are selected to detect TEC fluctuations associated with ionospheric disturbances over China, as shown in Figure 1. Dual-frequency GPS observations are sampled at 30 s intervals; the cut-off elevation angle is set at 15°; and the selected time period is from 2002 to 2012, although some data were missing.

First, original dual-frequency GPS phase and pseudo-range data from the 21 selected sites were preprocessed by removing gross errors and then detecting and repairing cycle slips using Melbourne-Wuebbena linear combinations, geometry-free linear combinations, and ionosphere-free linear combinations (for more details, refer to [40–44]). Then, we calculated the ROT along the signal

paths (epoch by epoch), which allowed us to obtain the corresponding TEC fluctuation index ROTI. Finally, we compared and analyzed the characteristics and regional differences in TEC fluctuations among the 21 GNSS tracking sites.

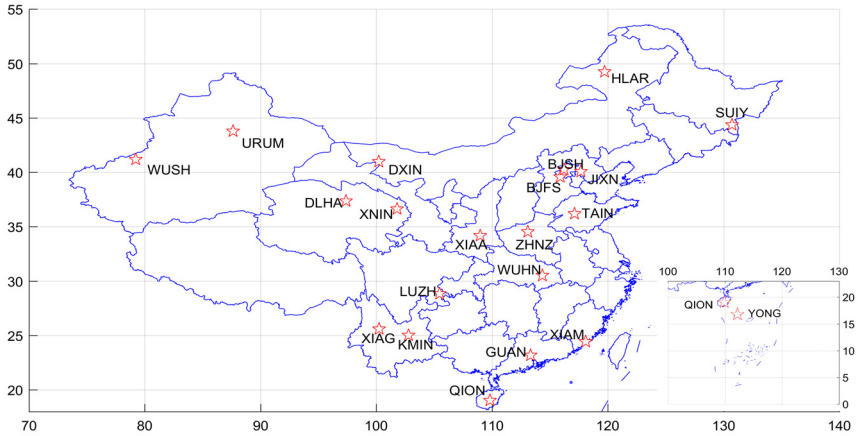

Figure 1. The locations of the 21 selected GNSS sites from CMONC.

3. Results and Discussion

In this section, we analyze and discuss the characteristics of TEC fluctuations over China during a solar cycle—the 11-year pattern from 2002 to 2012. First, 8 October 2003 (when there is an obvious ionospheric scintillation phenomenon) was selected as an example for demonstrating in detail the application of ROTI indices, and the spatial distribution characteristics of the ionospheric pierce point (IPP) were further analyzed according to the ROTI value of this day. Then, the temporal analysis results of ROTI at the QION and WUHN sites were taken as typical examples to illustrate the temporal variation characteristics of different latitudinal regions over China. Finally, to further investigate the characteristics of TEC fluctuations related to irregular ionospheric activities over China, the daily occurrence ratios of the TEC fluctuations of the 21 selected sites were further analyzed day by day from 2002 to 2012.

3.1. TEC Fluctuation Detection on 8 October 2003

To better show the application of ROTI to detecting ionospheric TEC fluctuations based on both GPS observation data from the QION site in Hainan provided by Crustal Movement Observation Network of China (CMONOC) and the ionospheric scintillation data from the FUKE site in Hainan provided by the Space Environment Monitoring Network of the Chinese Academy of Sciences, the time period was selected as 8 October 2003, which was during an obvious occurrence of scintillation in Hainan over the lower latitudes of China. QION is the GNSS tracking site nearest to the FUKE monitoring site, at a distance of less than 100 km, so the difference in ionospheric irregular activities between these sites may be considered slight.

Figures 2 and 3 (blue lines) show the time series of the ROT and ROTI derived from all of the observed GPS satellites at the QION site during the occurrence of ionospheric scintillation on 8 October 2003 (the results vary by universal time, UT). Figure 3 (red lines) shows the UT variation of the amplitude scintillation index S_4 of all observed GPS satellites at the FUKE monitoring site over the same time period. Local time (LT) can be approximately calculated by adding 8 h to the UT (LT = UT + 8). As depicted in Figure 2, affected by ionospheric scintillation, there were obviously rapid and random fluctuations of ROT that mainly occurred at night. Figure 3 shows that most of the observed satellites, such as the pseudo random noise code (PRN) 4, 7, 8, 20, 27, and 28, experienced obvious TEC fluctuations during the time period between 7 p.m. LT (pre-midnight) and

3 a.m. LT (post-midnight); there was an obvious loss of lock phenomena for satellites PRN 7 and 27. Significantly, very few TEC fluctuations were observed during any other time periods.

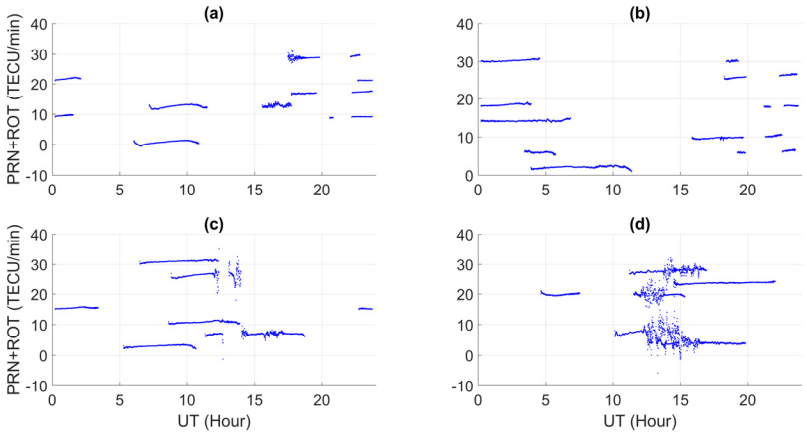

Figure 2. The time series of ROT for all of the observed GPS satellites at the QION site (8 October 2003). The vertical axis is the sum of the ROT value and PRN number of the corresponding satellite. The PRN numbers of each subfigure are as follows: (**a**) 1, 9, 13, 17, 21, 29; (**b**) 2, 6, 10, 14, 18, 26, 30; (**c**) 3, 7, 11, 15, 27, 31; (**d**) 4, 8, 20, 24, 28.

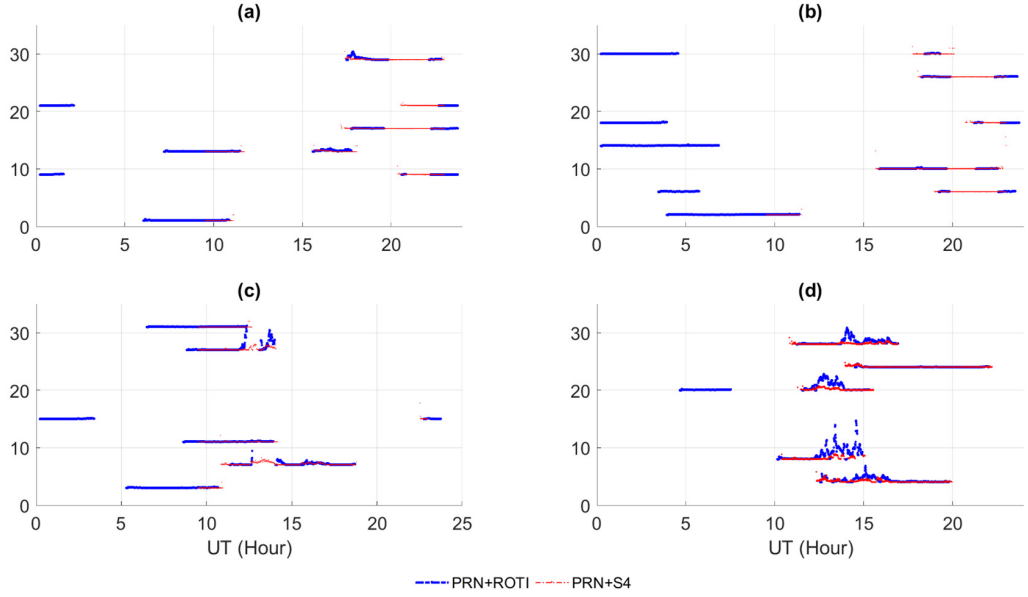

Figure 3. The time series of ROTI and amplitude scintillation index S_4 for all of the observed GPS satellites at the QION and FUKE sites (8 October 2003). The vertical axis is the sum of the ROTI or S_4 value and the PRN number of the corresponding satellite. The PRN numbers of each subfigure are as follows: (**a**) 1, 9, 13, 17, 21, 29; (**b**) 2, 6, 10, 14, 18, 26, 30; (**c**) 3, 7, 11, 15, 27, 31; (**d**) 4, 8, 20, 24, 28.

3.2. Spatial Distribution Analysis of ROTI over China on 8 October 2003

Based on the ROTI analysis over China during the occurrence of ionospheric scintillation on 8 October 2003, Figure 4 shows the spatial distribution of all IPP according to certain TEC fluctuation conditions along the propagating paths of all observed GPS signals from each site. To weaken the impact of the single-layer hypothesis on IPP as much as possible, a cut-off elevation angle of 30° is selected for IPP extraction in this section. As demonstrated in Figure 4, the spatial distribution of moderate or strong TEC fluctuations satisfying ROTI $\geq$ 0.5 is mainly located south of Guangdong, and very few TEC fluctuations are observed in other regions. The above phenomenon might be

closely related to the physical phenomena of irregular ionospheric activities, such as equatorial plasma bubbles induced by ionospheric scintillation, which might be affected by solar flares, geomagnetic storms, atmospheric waves and solar wind structures.

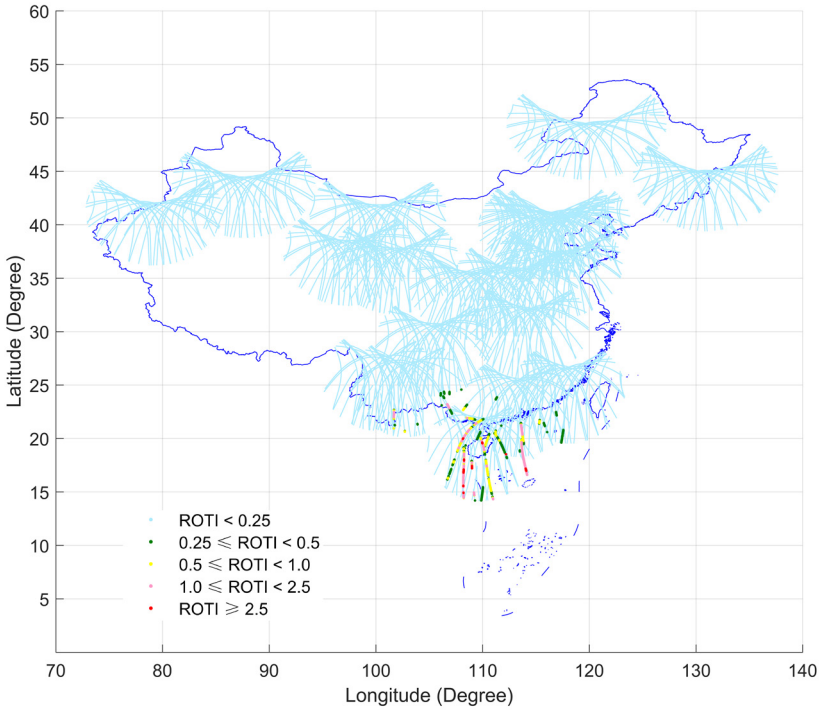

Figure 4. The spatial distribution of IPP according to the ROTI value for all of the observed GPS satellites from 20 sites across China (8 October 2003). The red point line refers to the IPP locations satisfying extremely strong TEC fluctuations ROTI $\geq$ 2.5; the pink point line refers to the IPP locations satisfying sub-strong TEC fluctuations 1.0 $\leq$ ROTI $<$ 2.5; the yellow point line refers to the IPP locations satisfying moderate TEC fluctuations 0.5 $\leq$ ROTI $<$ 1.0; the green point line refers to the IPP locations satisfying weak TEC fluctuations 0.25 $\leq$ ROTI $<$ 0.5; and the light blue point line refers to the IPP locations satisfying no TEC fluctuations ROTI $<$ 0.25.

3.3. Temporal Variation Analysis of ROTI at the QION and WUHN Sites

Figure 5 shows the time series of ROTI by day of year (DOY) at the QION site during 2012. The results show that most of the TEC fluctuations occurred during spring and autumn (equinox months) and that TEC fluctuations rarely occurred during summer and winter. Additionally, the daily occurrence of TEC fluctuations during the equinox months demonstrated obvious randomness, which makes it difficult to forecast irregular ionospheric activities (as described in Figure 5). Figure 6 shows the time series of ROTI in UT for all of the observed GPS satellites at the QION site in each season in 2012. Our results show that the TEC fluctuations mainly occurred between 7 p.m. LT (pre-midnight) and 3 a.m. LT (post-midnight) during the spring and autumn, primarily in the pre-midnight hours. The TEC fluctuations were much weaker during summer and winter than they were during spring and autumn. The weak TEC fluctuations in the summer mainly occurred during the nighttime. Interestingly, during the winter, the occurrence of weak TEC fluctuations could be observed not only at night but also during the day. The variations in the temporal characteristics of the TEC fluctuations over the Hainan region coincide with those of previous investigations of season- and nighttime-dependent variations in ionospheric scintillation characteristics over the north crest of the equatorial anomaly region in China's lower latitudes.

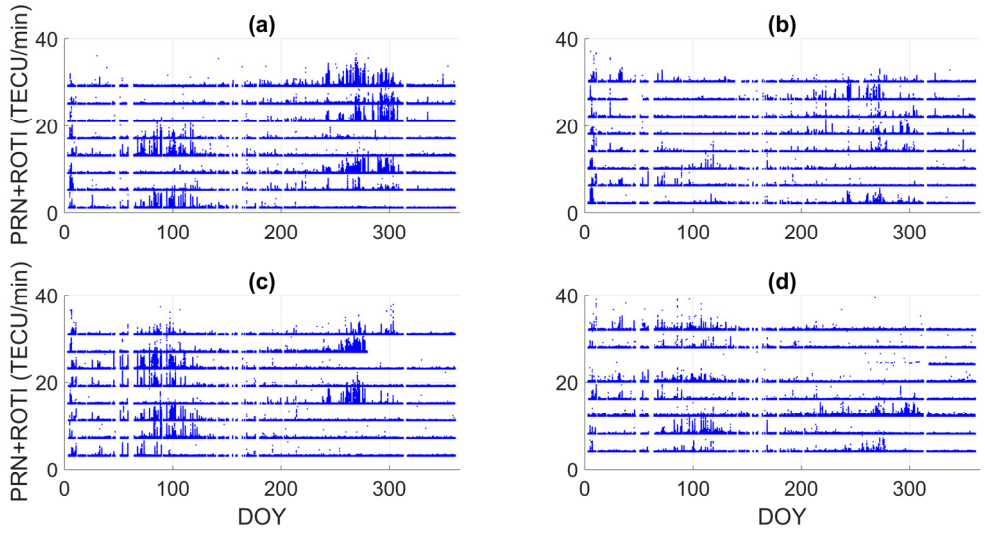

Figure 5. The time series of ROTI by day of year (DOY) for all of the observed GPS satellites at the QION site during 2012. The PRN numbers of each subfigure are as follows: (**a**) 1, 5, 9, 13, 17, 21, 25, 29; (**b**) 2, 6, 10, 14, 18, 22, 26, 30; (**c**) 3, 7, 11, 15, 19, 23, 27, 31; (**d**) 4, 8, 12, 16, 20, 28, 32.

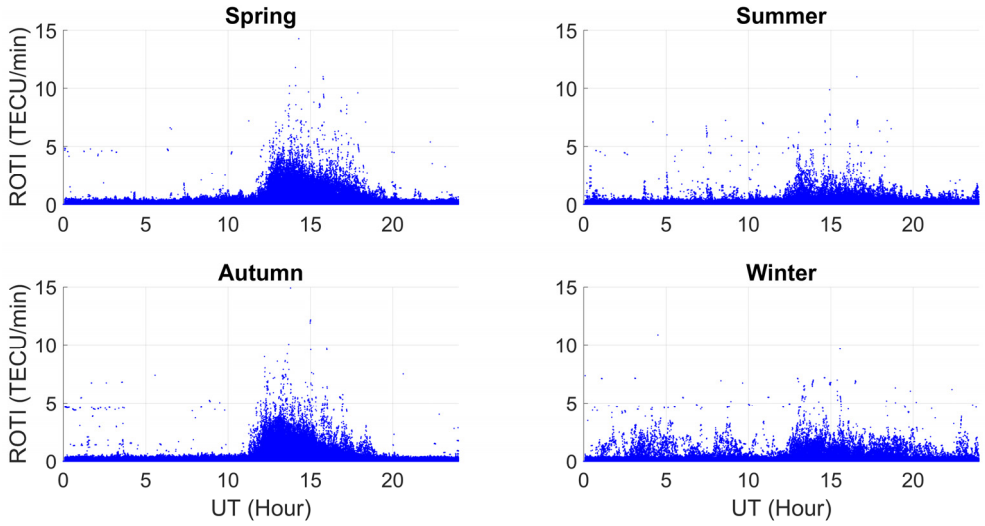

Figure 6. The time series of ROTI (in UT) for all of the observed GPS satellites at the QION site during the four seasons of 2012. The observation periods of each subfigure are as follows: spring: 1 March to 31 May; summer: 1 June to 31 August; autumn: 1 September to 30 November; winter: 1 December to 28 February.

Similar to Figure 5, Figure 7 shows the time series of ROTI by DOY at the WHUN site. The intensity of TEC fluctuations was significantly weaker at WUHN than at QION. Unlike QION, most of the TEC fluctuations over WUHN were observed in the spring, summer, and autumn. However, TEC fluctuations were only rarely observed during the winter. Thus, in contrast to QION, the season-dependent characteristics of TEC fluctuations over WUHN were significantly weaker. Moreover, the daily occurrence of TEC fluctuations demonstrated obvious randomness over WUHN. Figure 8 shows the distribution of TEC fluctuations (in UT) derived from all of the observed GPS satellites at the WHUN site during each season of 2012. Compared with the QION site, the LT time-dependent characteristics of the TEC fluctuations were weak and occasionally disappeared entirely during each season. This indicates that the occurrence of TEC fluctuations ceased to be a nighttime phenomenon.

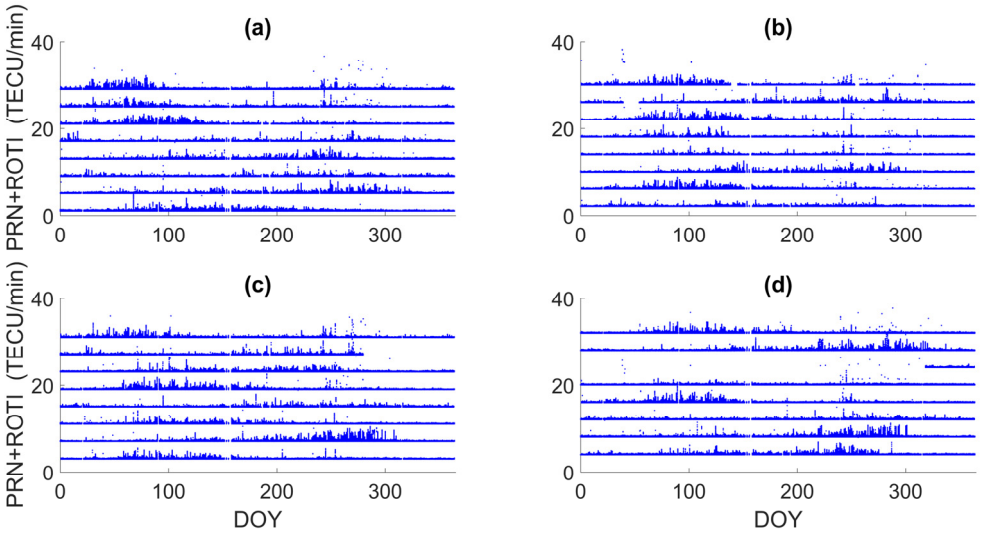

Figure 7. The time series of ROTI by day of year (DOY) for all of the observed GPS satellites at the WUHN site during 2012. The PRN numbers of each subfigure are as follows: (**a**) 1, 5, 9, 13, 17, 21, 25, 29; (**b**) 2, 6, 10, 14, 18, 22, 26, 30;(**c**) 3, 7, 11, 15, 19, 23, 27, 31; (**d**) 4, 8, 12, 16, 20, 28, 32.

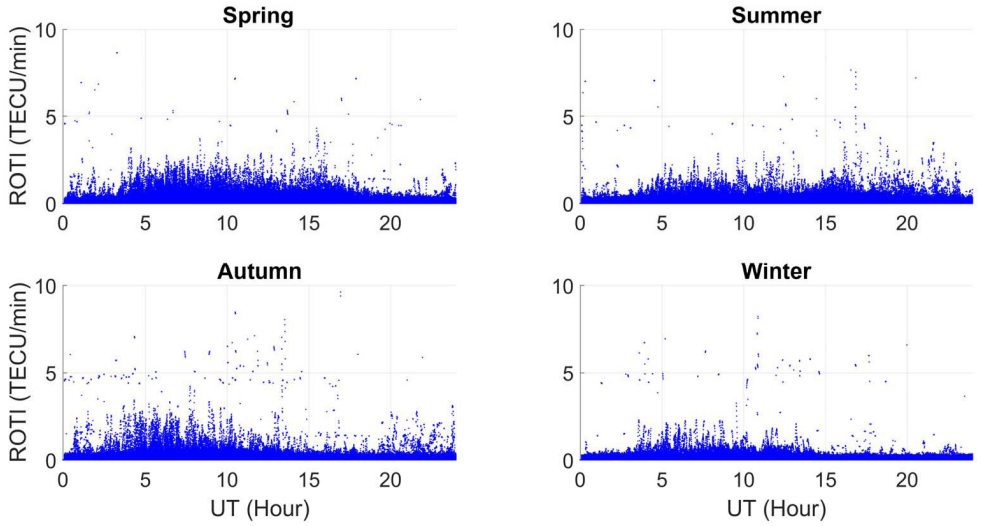

Figure 8. The time series of ROTI in UT for all of the observed GPS satellites at the WUHN site during the four seasons of 2012.

3.4. Daily Occurrence Ratio of TEC Fluctuations from 2002 to 2012

Typically, TEC fluctuations satisfying ROTI $\geq$ 0.5 indicate the occurrence of irregular ionospheric activities relevant to ionospheric scintillation [22]. In this study, we wanted to conduct a more in-depth quantitative analysis of the intensity of ionospheric disturbances and their occurrence ratio over China. As such, we based our analysis on the original ROTI value, which requires that the standard level of TEC fluctuations be preliminarily divided into three groups: weak if $0.25 \leq$ ROTI < 0.5; moderate if $0.5 \leq$ ROTI < 1; and strong if ROTI ≥ 1. The daily occurrence ratio is the ratio of the TEC fluctuation epoch numbers to all of the observed epoch numbers within one day.

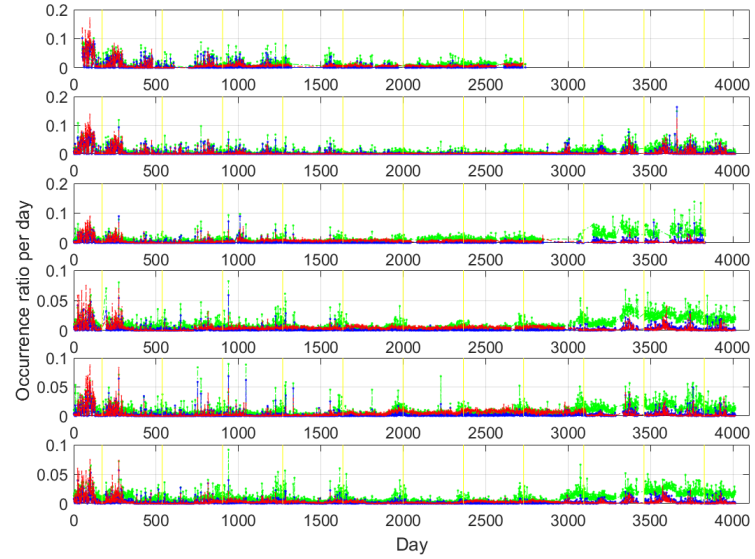

(**a**)

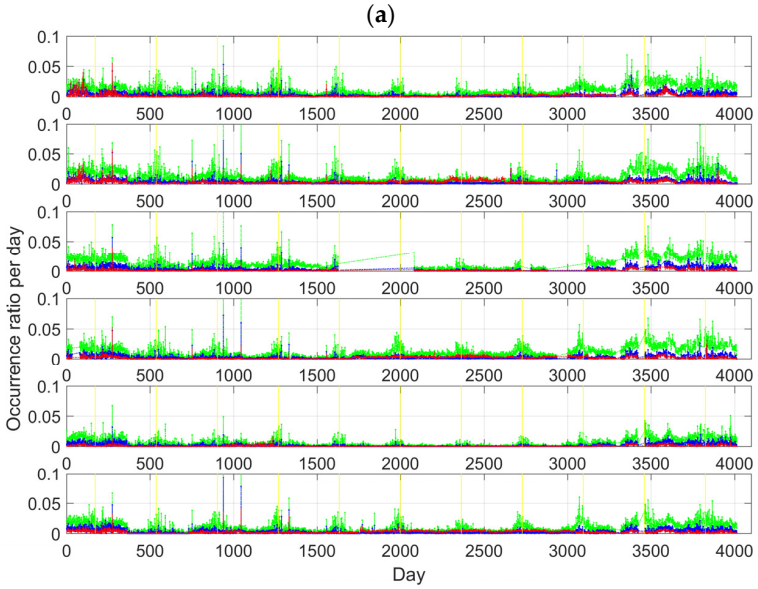

(**b**)

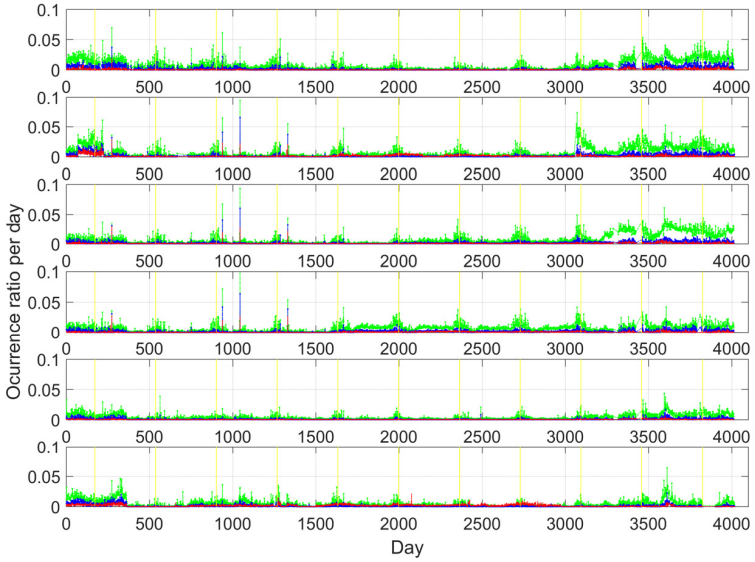

(**c**)

Figure 9. *Cont.*

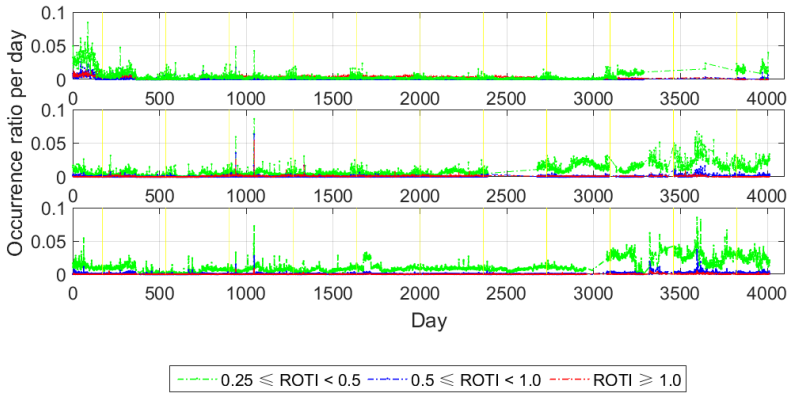

(**d**)

Figure 9. The daily occurrence ratio (by DOY) of the different-level TEC fluctuations at the 21 selected GNSS sites from 2002 to 2012. The green line represents the daily occurrence ratio of weak TEC fluctuations that satisfy $0.25 \leq \text{ROTI} < 0.5$; the blue line represents the daily occurrence ratio of moderate TEC fluctuations that satisfy $0.5 \leq \text{ROTI} < 1$; and the red line represents the daily occurrence ratio of strong TEC fluctuations that satisfy $\text{ROTI} \geq 1$. The straight yellow lines denote the day of the summer solstice of each year. The site names of each subfigure are as follows: (**a**) YONG, QION, GUAN, KMIN, XIAM, XIAG; (**b**) LUZH, WUHN, XIAA, ZHNZ, DLHA, TAIN; (**c**) XNIN, BJFS, BJSH, JIXN, WUSH, URUM; (**d**) DXIN, SUIY, HLAR.

Figure 9 shows the daily occurrence ratio of different-level TEC fluctuations day by day during a solar cycle (from 2002 to 2012) for each of the selected sites. All of the ROTI values satisfy the conditions detailed above. As shown in Figure 9, the long-periodic variation characteristics of ionospheric TEC fluctuation changes can be observed during a solar cycle, which is closely related to the years of the solar activity. Generally, the intensity of TEC fluctuations is observed to be much stronger during high solar activity than during low solar activity. Of the 11 years from 2002 to 2012, the occurrence frequencies and the intensity of TEC fluctuations reached the highest levels during 2002. Additionally, the intensity of TEC fluctuations was slightly weaker than that of 2002 during years of solar activity, such as 2011 and 2012, followed by 2003 and 2004. In other years, the intensity of TEC fluctuations became much smaller during periods of lower solar activity, such as from 2005 to 2010. Moreover, Figure 9 clearly indicates that strong TEC fluctuations that satisfy $\text{ROTI} \geq 1$ occurred mainly during the spring and autumn over most of the lower-latitude regions in southern China. Of those sites satisfying the strong ROTI requirements, the equinox characteristics in ionospheric disturbances were most significant at the YONG and QION sites. Equinox characteristics in ionospheric disturbances became slightly weaker at the GUAN, KMIN, XIAM, and XIAG sites, which is consistent with typical ionospheric scintillation characteristics over the north crest of the equatorial anomaly region in southern China. Significantly, the weakening of equinox characteristics in TEC fluctuations is related to not only the location but also the duration of solar activity during periods of high and low intensity. However, concurrent with the gradual weakening of equinox characteristics of TEC fluctuations, summer characteristics of TEC fluctuations gradually emerged at sites such as LUZH, WUHN, ZHNZ, and XIAA during the years of lower solar activity. The above phenomenon indicates that the weakening of equinox characteristics corresponds to the emergence of summer characteristics over southern China. The reason for the occurrence of TEC fluctuations during the June solstice over most of central China might be closely related to sporadic-E (Es) activity and medium-scale traveling ionospheric disturbances (MSTIDs) [45–47]. Additionally, the strong TEC fluctuation satisfying $\text{ROTI} \geq 1$ became increasingly rare with increasing latitude for all of the sites north of the LUZH site. Moreover, sites located in the higher mid-latitude areas, such as SUIY and HLAR, demonstrated weak or nonexistent summer characteristics in TEC fluctuations.

4. Conclusions

In this study, we investigated and analyzed the features of TEC fluctuations and their regional differences over China during a solar cycle, the 11-year pattern from 2002 to 2012. We utilized ROTI for the measurement of TEC fluctuations and correlated the measurements with irregular ionospheric activities (based on dual-frequency GPS data from 21 tracking stations provided by CMONC).

Our main conclusions are as follows.

(1) Strong TEC fluctuations were usually observed over low-latitude southern China and took on typical variations in temporal characteristics. Moreover, strong TEC fluctuations mainly occurred at night in the equinox months, especially during the years of higher solar activity. This phenomenon is consistent with the ionospheric scintillation characteristics over southern China.

(2) We observed that the intensity of equinox characteristics of TEC fluctuations weakened or disappeared entirely as the summer characteristics of TEC fluctuations gradually emerged. This is especially evident with increases in latitude, such as at the LUZH and WUHN sites, particularly during the years of lower solar activity. Under the above conditions, the occurrence of TEC fluctuations over China's mid-latitude regions is no longer restricted to nighttime but might also occur during the daytime.

(3) With respect to the lower mid-latitude regions of China, ionospheric TEC fluctuations mainly occur during the summer, such as at the ZHNZ site. Nevertheless, season-dependent variations in the characteristics of TEC fluctuations were rarely observed at the higher mid-latitude regions of northern China, such as at the SUIY and HLAR sites. Additionally, our results revealed that the season-dependent characteristics of TEC fluctuations weaken or disappear with increases in latitude. Relevant discussions of this phenomenon are still relatively rare, so our results contribute to the development of a more in-depth understanding of irregular ionospheric activities, specifically the characteristics and features that occur over China.

Acknowledgments: This work was partially supported by the Collaborative Precision Positioning Project funded by the Ministry of Science and Technology of the People's Republic of China (No. 2016YFB0501900) and the National Nature Science Foundation of China (Grant No. 41674022, 41231064, 41304034 and 41574033). We also acknowledge the funding support provided by the State Key Laboratory of Geodesy and Earth's Dynamics (the Institute of Geodesy and Geophysics, CAS) (No. SKLGED2014-3-1-E). The authors would like to extend their sincere gratitude to the Crustal Movement Observation Network of China for providing us with observational data. The authors are grateful to the Chinese Meridian Project for supplying relevant information concerning ionospheric scintillations. The authors are thankful to the IGS Multi-GNSS Experiment (http://mgex.igs.org) and International GNSS Monitoring and Assessment Service (iGMAS) for supplying the related prodution and services.

Author Contributions: Xifeng Liu and Yunbin Yuan provided the initial idea for this study; Xifeng Liu and Bingfeng Tan conceived and designed the experiment; Xifeng Liu and Min Li analyzed the results of the experiment; Xifeng Liu and Yunbin Yuan wrote the paper.

Conflicts of Interest: The authors declare no conflicts of interest.

Abbreviations

The following abbreviations are used in this manuscript:

CMONOC	Crustal Movement Observation Network of China
TEC	Total Electron Content
ROT	Rate of TEC
ROTI	Rate of TEC Index

References

1. Ji, S.; Chen, W.; Weng, D.; Wang, Z.; Ding, X. A study on cycle slip detection and correction in case of ionospheric scintillation. *Adv. Space Res.* **2013**, *51*, 742–753. [CrossRef]
2. Morton, Y.; Taylor, S.; Wang, J.; Jiao, Y.; Pelgrum, W. In L band ionosphere scintillation impact on GNSS receivers. In Proceedings of the IEEE Radio Science Meeting (USNC-URSI NRSM), 2013 US National Committee of URSI National, Boulder, CT, USA, 9–12 January 2013; p. 1.

3. Ghafoori, F.; Skone, S. Impact of equatorial ionospheric irregularities on GNSS receivers using real and synthetic scintillation signals. *Rad. Sci.* **2015**, *50*, 294–317. [CrossRef]
4. Kintner, P.; Ledvina, B.; De Paula, E. GPS and ionospheric scintillations. *Space Weather* **2007**, *5*, 83–104. [CrossRef]
5. Jacobsen, K.S.; Dahnn, M. Statistics of ionospheric disturbances and their correlation with GNSS positioning errors at high latitudes. *J. Space Weather Space Clim.* **2014**, *4*, A27. [CrossRef]
6. Tiwari, R.; Strangeways, H.J.; Tiwari, S.; Ahemad, A. Investigation of ionospheric irregularities and scintillation using TEC in high latitude. *Adv. Space Res.* **2013**, *52*, 1111–1124. [CrossRef]
7. Pi, X.; Mannucci, A.J.; Valant-Spaight, B.; Bar-Sever, Y.; Romans, L.J.; Skone, S.; Sparks, L.; Hall, G.M. Observations of global and regional ionospheric irregularities and scintillation using GNSS tracking networks. In Proceedings of ION 2013 Pacific PNT Meeting, Honolulu, HI, USA, 23–25 April 2013; pp. 752–761.
8. Cherniak, I.; Krankowski, A.; Zakharenkova, I. Observation of the ionospheric irregularities over the Northern Hemisphere: Methodology and service. *Rad. Sci.* **2014**, *49*, 653–662. [CrossRef]
9. Sieradzki, R.; Cherniak, I.; Krankowski, A. Near-real time monitoring of the TEC fluctuations over the Northern Hemisphere using GNSS permanent networks. *Adv. Space Res.* **2013**, *52*, 391–402. [CrossRef]
10. Jakowski, N.; Béniguel, Y.; De Franceschi, G.; Pajares, M.H.; Jacobsen, K.S.; Stanislawska, I.; Tomasik, L.; Warnant, R.; Wautelet, G. Monitoring, tracking and forecasting ionospheric perturbations using GNSS techniques. *J. Space Weather Space Clim.* **2012**, *2*, 22. [CrossRef]
11. Pi, X.; Mannucci, A.; Lindqwister, U.; Ho, C. Monitoring of global ionospheric irregularities using the worldwide GPS network. *Geophys. Res. Lett.* **1997**, *24*, 2283–2286. [CrossRef]
12. Wang, M.; Ding, F.; Wan, W.; Ning, B.; Zhao, B. Monitoring global traveling ionospheric disturbances using the worldwide GPS network during the October 2003 storms. *Earth Planets Space* **2007**, *59*, 407–419. [CrossRef]
13. Shang, S.; Shi, J.; Zhang, B.; Xiao, W.; Wu, S. Characteristics of ionospheric irregularities near Eastern Asia based on GPS observations. *Chin. J. Rad. Sci.* **2014**, *29*, 627–633. (In Chinese)
14. Yuan, Y.; Ou, J. Auto-covariance estimation of variable samples (ACEVS) and its application for monitoring random ionospheric disturbances using GPS. *J. Geodesy.* **2001**, *75*, 438–447. [CrossRef]
15. Li, G.; Ning, B.; Yuan, H. Analysis of ionospheric scintillation spectra and TEC in the Chinese low latitude region. *Earth Planets Space* **2007**, *59*, 279–285. [CrossRef]
16. Tang, L.; Yang, X.; Kan, Z.; Li, Q. Lane-level road information mining from vehicle GPS trajectories based on naïve bayesian classification. *ISPRS Int. J. Geo-Inf.* **2015**, *4*, 2660–2680. [CrossRef]
17. Xie, X.; Wong, K.B.-Y.; Aghajan, H.; Veelaert, P.; Philips, W. Inferring directed road networks from GPS traces by track alignment. *ISPRS Int. J. Geo-Inf.* **2015**, *4*, 2446–2471. [CrossRef]
18. Li, J.; Zhang, Y.; Wang, X.; Qin, Q.; Wei, Z.; Li, J. Application of GPS trajectory data for investigating the interaction between human activity and landscape pattern: A case study of the Lijiang River Basin, China. *ISPRS Int. J. Geo-Inf.* **2016**, *5*, 104. [CrossRef]
19. Ranacher, P.; Brunauer, R.; van der Spek, S.; Reich, S. What is an appropriate temporal sampling rate to record floating car data with a GPS? *ISPRS Int. J. Geo-Inf.* **2016**, *5*, 1. [CrossRef]
20. Wu, T.; Xiang, L.; Gong, J. Updating road networks by local renewal from GPS trajectories. *ISPRS Int. J. Geo-Inf.* **2016**, *5*, 163. [CrossRef]
21. Basu, S.; Groves, K.M.; Quinn, J.M.; Doherty, P. A comparison of TEC fluctuations and scintillations at Ascension Island. *J. Atmos. Sol.-Terr. Phys.* **1999**, *61*, 1219–1226. [CrossRef]
22. Yang, Z.; Liu, Z. Correlation between ROTI and ionospheric scintillation indices using Hong Kong low-latitude GPS data. *GPS Solut.* **2015**, *20*, 1–10. [CrossRef]
23. Mungufeni, P.; Jurua, E.; Habarulema, J.B.; Katrini, S.A. Modelling the probability of ionospheric irregularity occurrence over African low latitude region. *J. Atmos. Sol.-Terr. Phys.* **2015**, *128*, 46–57. [CrossRef]
24. Shagimuratov, I.; Krankowski, A.; Ephishov, I.; Cherniak, Y.; Wielgosz, P.; Zakharenkova, I. High latitude TEC fluctuations and irregularity oval during geomagnetic storms. *Earth Planets Space* **2012**, *64*, 521–529. [CrossRef]
25. Sieradzki, R.; Paziewski, J. Study on reliable GNSS positioning with intense TEC fluctuations at high latitudes. *GPS Solut.* **2016**, *20*, 553–563. [CrossRef]
26. Deng, B.; Huang, J.; Kong, D.; Xu, J.; Wan, D.; Lin, G. Temporal and spatial distributions of TEC depletions with scintillations and ROTI over south China. *Adv. Space Res.* **2015**, *55*, 259–268. [CrossRef]

27. Deng, B.; Huang, J.; Liu, W.; Xu, J.; Huang, L. GPS scintillation and TEC depletion near the northern crest of equatorial anomaly over south China. *Adv. Space Res.* **2013**, *51*, 356–365. [CrossRef]
28. Huang, L.; Wang, J.; Jiang, Y.; Chen, Z.; Zhao, K. A study of GPS ionospheric scintillations observed at Shenzhen. *Adv. Space Res.* **2014**, *54*, 2208–2217. [CrossRef]
29. Ji, S.; Chen, W.; Weng, D.; Wang, Z. Characteristics of equatorial plasma bubble zonal drift velocity and tilt based on Hong Kong GPS CORS network: From 2001 to 2012. *J. Geophys. Res. Space Phys.* **2015**, *120*, 7021–7029. [CrossRef]
30. Li, G.; Ning, B.; Liu, L.; Abdu, M.A.; Wan, W.; Hu, L. Shear in the zonal drifts of 3-m irregularities inside Spread-F plumes observed over Sanya. *J. Geophys. Res. Space Phys.* **2016**, *120*, 8146–8154. [CrossRef]
31. Liu, K.; Li, G.; Ning, B.; Hu, L.; Li, H. Statistical characteristics of low-latitude ionospheric scintillation over China. *Adv. Space Res.* **2015**, *55*, 1356–1365. [CrossRef]
32. Liu, L.; Chen, Y.; Le, H.; Ning, B.; Wan, W.; Liu, J.; Hu, L. A case study of postmidnight enhancement in F-layer electron density over Sanya of China. *J. Geophys. Res. Space Phys.* **2013**, *118*, 4640–4648. [CrossRef]
33. Liu, L.; He, M.; Yue, X.A.; Ning, B.; Wan, W. Ionosphere around equinoxes during low solar activity. *J. Geophys. Res.* **2010**, *115*, A9. [CrossRef]
34. Liu, Z.; Xu, R.; Morton, Y.; Xu, J.; Pelgrum, W.; Chen, W.; Ding, X. A comparison of GNSS-based ionospheric scintillation observation in north and south Hong Kong. *ION Pac. PNT* **2013**, *8900*, 694–705.
35. Shang, S.; Shi, J.; Guo, S. Ionospheric scintillation monitoring and preliminary statistic analysis over Hainan region. *Chin. J. Space Sci.* **2005**, *25*, 23–28. (In Chinese)
36. Shang, S.; Shi, J.; Guo, S. Morphological study of L-band ionospheric scintillation in the equatorial region. *Chin. J. Radio Sci.* **2006**, *21*, 410–415. (In Chinese)
37. Shi, J.; Wang, G.; Reinisch, B.; Shang, S.; Wang, X.; Zherebotsov, G.; Potekhin, A. Relationship between strong range spread F and ionospheric scintillations observed in Hainan from 2003 to 2007. *J. Geophys. Res.* **2011**, *116*, A08306. [CrossRef]
38. Xiong, B.; Wan, W.X.; Ning, B.Q.; Yuan, H.; Li, G.Z. A comparison and analysis of the S-4 index, C/N and ROTI over Sanya. *Chin. J. Geophys.* **2007**, *50*, 1639–1648. (In Chinese) [CrossRef]
39. Zou, Y. Ionospheric scintillations at Guilin detected by GPS ground-based and radio occultation observations. *Adv. Space Res.* **2011**, *47*, 945–965. [CrossRef]
40. Zhang, B. Three methods to retrieve slant total electron content measurements from ground-based GPS receivers and performance assessment. *Rad. Sci.* **2016**, *51*, 972–988. [CrossRef]
41. Zhang, B.; Teunissen, P. Characterization of multi-GNSS between-receiver differential code biases using zero and short baselines. *Chin. Sci. Bull.* **2015**, *60*, 1840–1849. [CrossRef]
42. Zhang, B.; Yuan, Y.; Chai, Y.Q. If-based GPS long-baseline ambiguity resolution with the aid of atmospheric delays determined by PPP. *J. Navig.* **2016**, *69*, 1278–1296. [CrossRef]
43. Zhang, B.C.; Ou, J.K.; Yuan, Y.B.; Li, Z.S. Extraction of line-of-sight ionospheric observables from GPS data using precise point positioning. *Sci. China Earth Sci.* **2012**, *55*, 1919–1928. [CrossRef]
44. Li, Z.; Yuan, Y.; Li, H.; Ou, J.; Huo, X. Two-step method for the determination of the differential code biases of Compass satellites. *J. Geod.* **2012**, *86*, 1059–1076. [CrossRef]
45. Li, G.; Ning, B.; Liu, L.; Wan, W.; Hu, L.; Zhao, B.; Patra, A. Equinoctial and june solstitial F-region irregularities over Sanya. *Indian J. Rad. Space Phys.* **2012**, *41*, 184–198.
46. Yang, J.; Huang, J.; Jie, X.; Deng, B.; Quan, H. Study of Sporadic E layers based on occultation data observed by FY-3C satellite. *Chin. J. Space Sci.* **2016**, *36*, 305–311. (In Chinese)
47. Ding, F.; Wan, W.; Xu, G.; Yu, T.; Yang, G.; Wang, J. Climatology of medium-scale traveling ionospheric disturbances observed by a GPS network in central China. *J. Geophys. Res. Atmos.* **2011**, *116*, 412–419. [CrossRef]